0888-8809/03/$15.00/0
Printed in U.S.A.

Molecular Endocrinology 17(10):2070–2083

doi: 10.1210/me.2003-0146

Estrogen Receptor-Dependent Genomic Responses in the Uterus Mirror the Biphasic Physiological Response to Estrogen

SYLVIA CURTIS HEWITT, BONNIE J. DEROO, KATHERINE HANSEN, JENNIFER COLLINS, SHERRY GRISSOM, CYNTHIA A. AFSHARI, AND KENNETH S. KORACH

Receptor Biology Section (S.C.H., B.J.D., K.H., K.S.K.) and Microarray Group (J.C., S.G., C.A.A.), National Institute of Environmental Health Sciences, National Institutes of Health, Research Triangle Park, North Carolina 27709

The physiological responses of the rodent uterus to acute estrogen (E) dosing can be divided into early and late events. Examples of early responses include increased RNA transcription, hyperemia, and water imbibition 2 and 6 h following E administration respectively, whereas later responses include cycles of DNA synthesis and mitosis of epithelial cells beginning 10 and 16 h after E. The development of estrogen receptor (ER) knockout (ERKO) mice, combined with microarray technology, has allowed us to design a genomic approach to study the acute response of the rodent reproductive tract to E. To determine whether early and late biological responses are correlated with altered regulation of a single set of genes or distinct sets of genes characteristic of early and late responses, uterine RNA was obtained from ovariectomized mice that were treated with vehicle or with estradiol for 2 h (early) or 24 h (late). Samples were also prepared from identically treated mice that lacked either ERα (αERKO) or ERβ (βERKO) to address the relative contributions of the ERs in the uterine responses. Microarray analysis of the relative expression of 8700 mouse cDNAs indicated distinct clusters of genes that were regulated both positively and negatively by E in the early or late phases as well as clusters of genes regulated at both times. Both early and late responses by the βERKO samples were indistinguishable from those of WT samples, whereas the αERKO showed little change in gene expression in response to E, indicating the predominant role for ERα in the genomic response. Further studies indicated that the genomic responses in samples from intermediate time points (6 h, 12 h) fall within the early or late clusters, rather than showing unique clusters regulated in the intermediary period. The use of this genomic approach has illustrated how physiological responses are reflected in genomic patterns. Furthermore, the identification of functional gene families that are regulated by E in the uterus combined with the utilization of genetically altered experimental animal models can help to uncover and define novel mechanisms of E action. (*Molecular Endocrinology* 17: 2070–2083, 2003)

THE RODENT REPRODUCTIVE tract must respond properly to precisely timed physiological signals in order for pregnancy to be established and maintained. Immediately before ovulation, serum estrogen (E) surges, and in response to this surge the uterine tissues exhibit well-characterized physiological and biochemical responses. These observed responses have been divided into events that occur early, within the first hours after E elevation, and subsequent responses that follow up to 24 h after the E administration. Thus, this acute and rapid response of the uterus has been described as biphasic in nature, as summarized in Table 1 (1, 2). Early events include nuclear estrogen receptor (ER) occupancy, transcription of early phase genes such as c-*fos*, fluid uptake (termed water imbibition), hyperemia, and infiltration of immune system cells such as macrophages and eosinophils into the uterine tissue (3, 4). Later phase responses include the transcription of late phase genes such as *lactoferrin*, increase in uterine wet weight, further accumulation of immune system cells, the development of the epithelial layer into columnar secretory epithelial cells, and subsequent mitosis, which occurs principally in the epithelial layer (5). Although these responses have been well characterized, several questions remain that can be addressed with the available global genomic expression technologies. One such question is whether early and late responses are the result of altered regulation of a single set of genes or whether there are distinct gene clusters characteristic of both the early and late responses. Secondly, whereas a handful of E-responsive genes have been identified and well characterized, the

Abbreviations: *BAD*, Bcl-associated death promoter; Ct, crossing threshold; Cy3 or 5, cyanine 3 or 5; *Cyr61*, cysteine-rich protein 61; DNase, deoxyribonuclease; E, estrogen; ER, estrogen receptor; ERKO, ER knockout; αERKO, mice that lacked ERα; βERKO, mice that lacked ERβ; HDAC5, histone deacetylase 5; HRP, horseradish peroxidase; ICI, anti-estrogen ICI 182,780; IGFBP, IGF binding protein; IκBα, inhibitor of NF-κB; LE, luminal epithelium; MAD2, mitotic arrest-deficient, homolog-like 2; NIEHS, National Institute of Environmental Health Sciences; NF-κB, nuclear factor-κB; ovx, ovariectomized; *SOX4*, SRY box-containing gene 4; Str, stromal; WT, wild-type.

functions associated with these genes are not in themselves sufficient to describe the dramatic biphasic biological responses observed. A more global gene discovery approach might identify novel targets and coordinated regulation of pathways by E and greatly increase our understanding of the biological response of the uterus to ovarian steroids. Finally, in such a study, the relationship between early and late gene clusters could be examined as well as the question of whether the early responses "prime" later responses. Therefore, using microarray technology, we compared the global expression pattern of uterine RNA from ovariectomized (ovx) control animals to those of ovx animals treated with estradiol for various intervals between 30 min and 24 h. Distinct clusters corresponding to early and late phase responses were apparent in the analysis of the relative gene expression in these samples indicating the biphasic physiological response is mirrored by a biphasic genomic response. The genomic response in mice that lacked either ERα [αERKO (αER knockout)] or ERβ (βERKO) examined after 2 h (early) or 24 h (late) of E treatment illustrated the requirement for ERα in both early and late responses to E.

RESULTS

Microarray Analysis of Early and Late Genomic Responses

Samples were prepared from wild-type (WT), αERKO, or βERKO uterine tissue after ovariectomy and treatment with vehicle or estradiol for 2 or 24 h, and then labeled and hybridized pair wise on multiple chip replicates. As we have previously reported, the αERKO uterine tissue is not biologically equivalent to the WT and βERKO, as the αERKO uterus does not respond to E and remains hypoplastic and immature (6). For this reason, pair-wise hybridizations were carried out as described in Table 2, within each ER genotype, to minimize effects resulting from biological differences in the uterine tissues. Lists of differentially expressed genes at the 99% confidence levels were created from each of the four replicate array hybridizations of each sample pair. Differentially expressed genes were clustered and displayed in dendograms, with red representing up-regulated genes, and green representing down-regulation (Fig. 1). WT and βERKO samples exhibited distinct clusters of genes whose expression changed at either 2 or 24 h, as well as clusters of genes regulated at both time points, which indicated the gene changes mirror the biphasic nature of the uterine physiological response. Significantly more genes were regulated at both 2 and 24 h in WT and βERKO samples than in the αERKO samples.

The expression patterns of the WT and βERKO were generally indistinguishable (Fig. 1), and any differences were comparable to the differences observed within the four biological replicate experiments using WT samples (not shown). Interestingly, although there was a minimal genomic response in the αERKO samples (Fig. 1), the cluster analysis indicated that the αERKO response at 2 or 24 h was more similar to that of the WT at the same time point than to the other αERKO time point. Specifically, the αERKO 2 h treatment clustered with WT 2 h rather than with αERKO 24 h (Fig. 1). This indicated that a biphasic genomic response also occurs in the absence of ERα, although the response is greatly attenuated relative to the WT and not sufficient for biological responses of uterine growth. In addition to the decreased number of gene changes, the intensity of responsiveness of the genes in the αERKO (depicted by the intensity of the color in the figure) was diminished compared with WT and βERKO, indicating the need for ERα to mount a full response to estradiol. In the tables published as supplemental data on The Endocrine Society's Journals Online web site at http://mend.endojournals.org, supplemental Table 1 lists the significant gene changes identified at the 99% confidence level in at least 75% of the hybridizations for the WT, αERKO, or βERKO samples. The WT list is a compilation of four independent experiments, the αERKO list from two experiments, whereas the βERKO list is generated from a single experiment.

Treatment of WT, βERKO, or αERKO mice with the antiestrogen ICI 182,780 (ICI) 30 min before estradiol injection inhibited the genomic responses at both

Table 1. Hours after Acute E Dosing

24	Second wave of mitosis, second peak of DNA synthesis, peak of dry weight increase
16	First wave mitosis, peak of DNA synthesis
10	Second increase in RNA Pol II activity, DNA synthesis begins
8	Second peak of ER nuclear occupancy
6	Water Imbibition
4	Protein synthesis increasing
2	RNA synthesis increasing, peak of ER nuclear occupancy
1	ER-E complex tightly bound in nucleus, RNA Pol II activity increases
0	

Table 2. Pairwise Hybridizations for Microarray Analysis

	2 h E	24 h E
WT	WT Veh *vs.* WT 2 h E	WT Veh *vs.* WT 24 h E
αERKO	αERKO Veh *vs.* αERKO 2 h E	αERKO Veh *vs.* αERKO 24 h E
βERKO	βERKO Veh *vs.* βERKO 2 h E	βERKO Veh *vs.* βERKO 24 h E

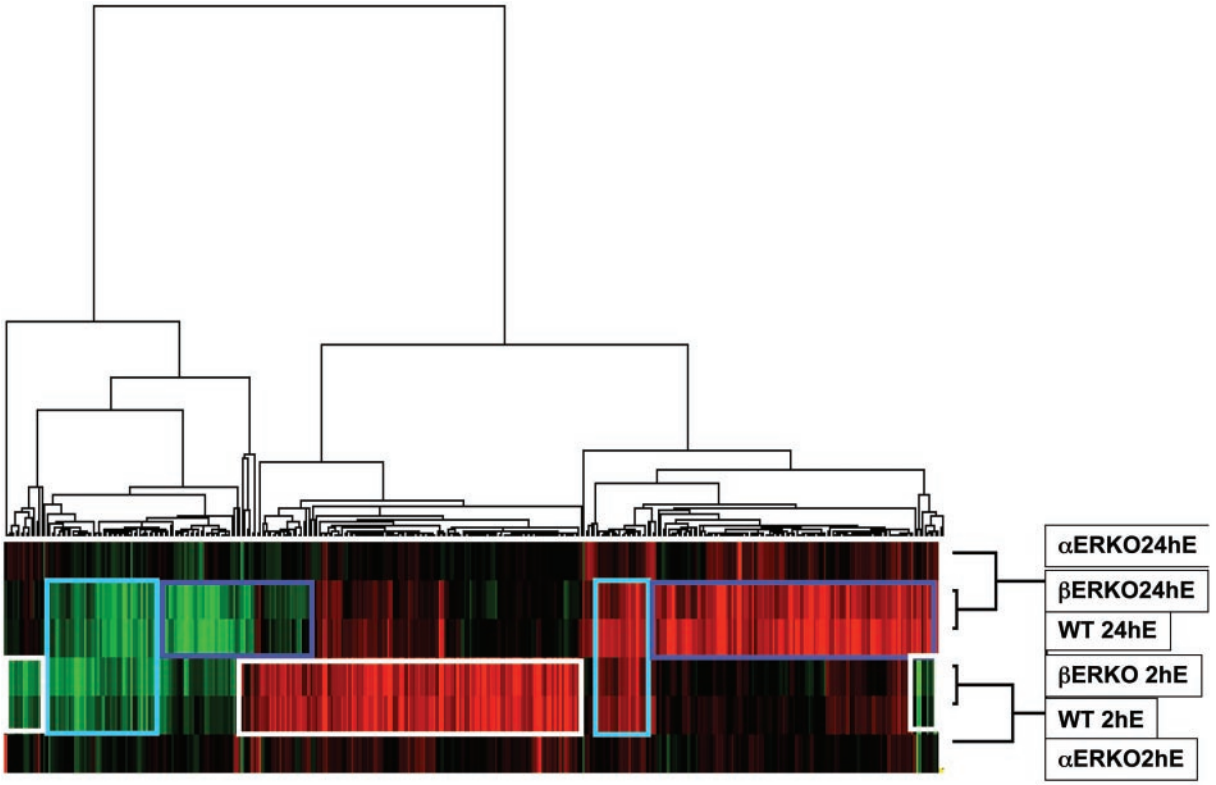

Fig. 1. Cluster Analysis of Microarray Data Indicates a Biphasic Genomic Response that Is ERα Dependent

Data obtained from microarray analysis as described in *Materials and Methods* were used to generate a cluster analysis. Each *vertical line* represents a single gene. Genes that were increased by estradiol treatment relative to vehicle treatment are indicated by *red*, with relative intensity representing degree of regulation. Down-regulated genes are similarly shown in *green*. The "2" or "24" indicates gene changes of vehicle compared with 2 h or 24 h of E treatment, respectively. Data are positioned according to the similarity in response, with most similar gene change patterns adjacent to one another. The *lengths of the lines* in the tree indicate the similarity in regulatory pattern for each gene, with *shorter length* indicating more similarity. *Boxes* around clusters highlight the early (*white boxes*) and late (*dark blue boxes*) responses as well as those that span both (*light blue boxes*). The WT data were obtained from four independent biological replicate experiments, the αERKO from two independent biological replicate experiments, and the βERKO from one experiment. Each experiment included four replicate hybridizations.

phases, as shown in Fig. 2. Note that the ICI-treated samples were nevertheless most similar to their time point counterparts of E treatment, indicating they retain some responsiveness. The ICI-mediated attenuation was most profound in the WT and βERKO samples, again illustrating the overwhelming dependence of the genomic response of the uterus to estradiol on classical ERα-mediated mechanisms.

To determine whether the genomic responses at time points between 2 and 24 h would reveal clusters of genes unique to the intermediate times, additional WT uterine RNA samples from animals treated with estradiol for 30 min, 2 h, 6 h 12 h, and 24 h were prepared and analyzed. Interestingly, as shown in Fig. 3, the majority of the changes in gene expression at the intermediate times occur within the previously identified early (2 h) or late (24 h) clusters, although the intensity of response was greater for certain genes at the intermediate times (indicated by the relative intensity of the colors). The response after 30 min was minimal, including only six genes, some not previously described as E regulated such as IκBα [inhibitor of nuclear factor (NF-κB)] and p21 (see Table 3 and supplemental Table 1).

Uterine genes previously characterized as E responsive were seen in the microarray data set as were many genes not previously identified as E regulated (Table 3). These included genes involved in chromatin structure, cell cycle regulation, the thioredoxin system, Wnt signaling, keratinization or cornification, and apoptosis (Table 3). For this study, we have initially focused on verifying the observed regulation of cell cycle modulators to gain insight into their roles in the uterine responses to E.

Estradiol Regulates Cell Cycle Modulators

The patterns of transcriptional regulation of several modulators of cell cycle progression by acute E treatment (Table 3) suggested their potential roles in the timing of the observed uterine biological response. For example, transcription of *p21*, which

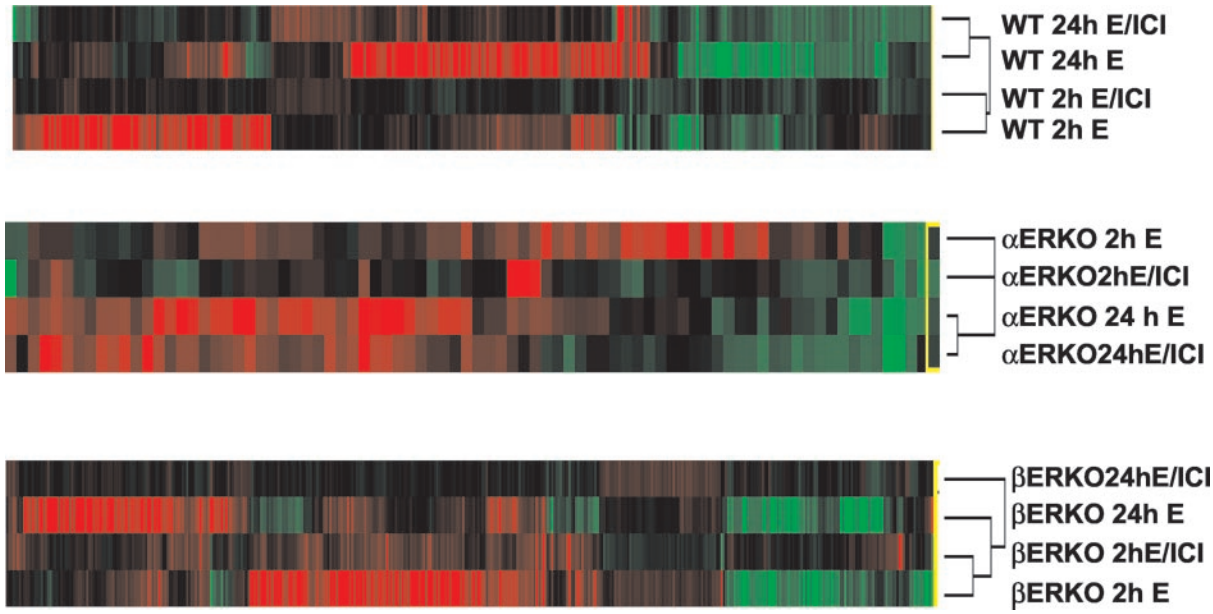

Fig. 2. Antiestrogen ICI Inhibits the Genomic Responses to Estradiol

Separate dendograms were generated for each ER genotype using the data in Fig. 1 and data from samples treated with ICI with estradiol. The hierarchical trees for the genes are not included in this figure. The placement of genes along the cluster is determined by their regulatory patterns; thus, the order of the genes on the three dendograms cannot be compared.

causes delay of S phase progression (7), was induced rapidly at 30 min, whereas the transcription of *cyclin G1*, which is important for progression into S phase (8), was increased after 12 h as DNA synthesis is beginning (see Table 1). Real-time RT-PCR analysis was used to verify the regulation of cell cycle genes observed in the microarray study as well as to examine the regulation of other cell cycle modulators known to be expressed in the uterus. As shown in Fig. 4A, RT-PCR analysis, in agreement with the microarray analysis, showed that induction of *p21* transcript peaked at 2 h and again at 12 h, and diminished by 24 h. RT-PCR analysis also verified that transcripts of *cyclins G1* as well as *E1*, a G1/S cyclin (9), were induced after acute E treatment (Fig. 4A), but with a timing that lagged compared with that of *p21*, as these cyclin transcripts continued increasing after the decrease of *p21* after 12 h. Transcripts of *cyclin D1*, although detected in the uterine samples by RT-PCR, showed little variation in levels after E treatment (Table 4), with a 1.6-fold increase at 12 h. Mitotic arrest-deficient, homolog-like 2 (*MAD2*), which functions in mitotic spindle assembly at the G2/M checkpoint (10, 11), is rapidly and robustly induced, peaking at 2 h with almost 20-fold induction (Fig. 4A), yet later decreases, mirroring the trend observed by microarray analysis (compare with Table 3). Pretreatment with ICI prevented E-mediated induction of all of these cell cycle regulators (Fig. 4B), additionally, none of these transcripts was seen in the microarray analysis of the αERKO samples (see supplemental Table 1) indicating that E regulation of these transcripts involves the classical ER-mediated mechanism. Generally, we observed that the microarray analysis consistently underestimated the degree of regulation when compared with RT-PCR analysis. For example, the microarray analysis indicated that *MAD2* transcript level increased 4.3-fold after 2 h of E, whereas RT-PCR analysis indicated the increase was nearly 20-fold. This underestimation has been previously reported as common in comparison of microarray analysis to other methods (12).

To determine whether the pattern of RNA regulation of these cell cycle modulators was reflected at the protein level, proteins were extracted from identically treated uterine samples and analyzed by Western blot for expression of p21, cyclin E1, or MAD2 proteins. The level of p21 protein showed a slight increase at 2 h (not shown) but was significantly increased by 6 h (Fig. 5A) and peaked at 12 h, with significant expression remaining at 24 h. ICI pretreatment prevented this increase in protein. Although *p21* transcription began increasing 30 min following E treatment (Fig. 4A), p21 protein expression did not increase until 6 h (Fig. 5A), but both the transcript and the protein peaked at 12 h. The degree of regulation at the protein level was not as robust, indicating posttranslational regulation may also occur. Cyclin E1 protein could be detected as a weak signal in the 6-h sample (Fig. 5B) and increased in the 12- and 24-h samples, indicating that protein expression mirrored that of the transcript. Pretreatment with ICI reduced the cyclin E1 expression only at 24 h, however. The profile of MAD2 protein expression by Western blot did not corre-

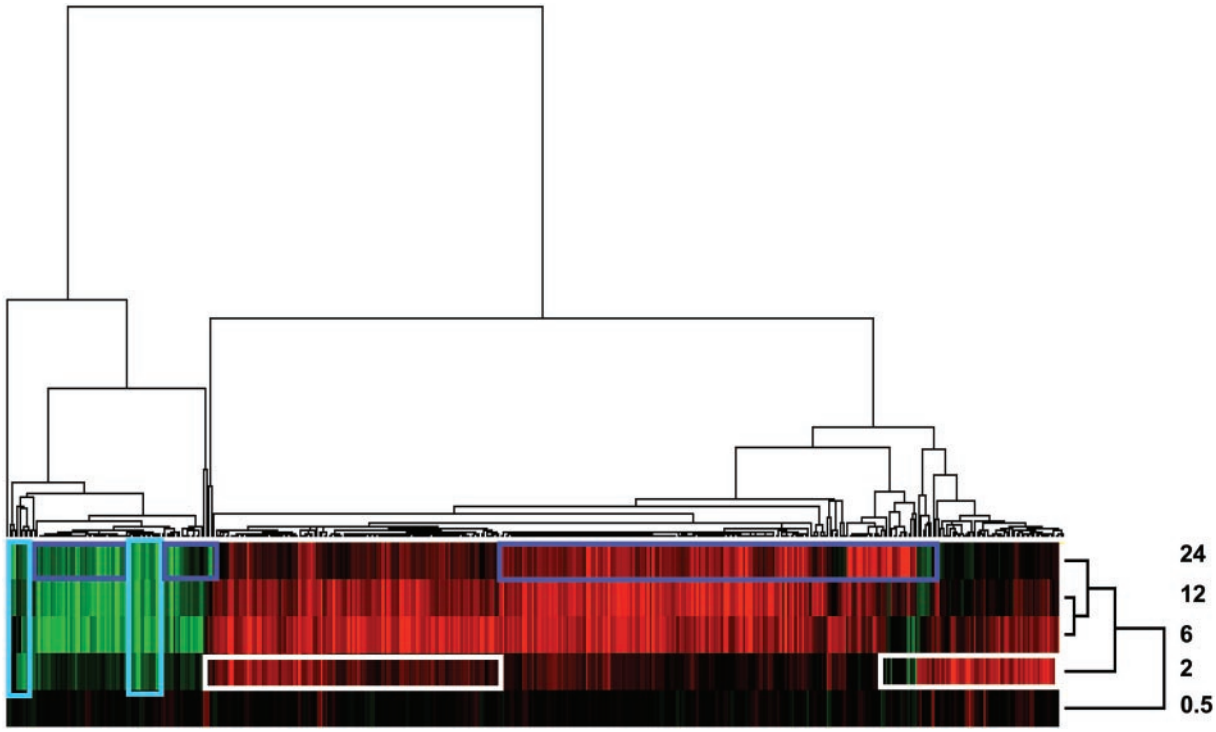

Fig. 3. Cluster Analysis of the Time Course of Response to Estradiol Indicates Intervening Genomic Responses Fall within Early or Late Gene Clusters

As described in the text, uterine RNA from WT mice treated with estradiol for 30 min or 2, 6, 12, or 24 h was compared with vehicle control by microarray. The *boxes* indicate the early (*white*) and late (*dark blue*) clusters as in Fig. 1. The data from the 2- and 24-h time points were obtained in four independent biological replicate experiments, whereas data from all other time points were obtained from a single experiment.

spond to the RNA profile. MAD2 protein was present in ovx uterine samples (Fig. 5C) but increased at 30 min, decreased at 2 h, then began increasing once more at 12–24 h following E treatment. Pretreatment with ICI decreased MAD2 levels below that seen in the vehicle sample. In this case, the timing as well as the degree of the regulation at the protein level did not correlate with that observed at the transcriptional level, indicating that posttranscriptional regulation may occur as well.

To determine which uterine cells express p21 protein, cross sections from samples used in the RT-PCR and Western blot analysis were stained with p21 antibody. Although p21 was detected by Western blots using whole uterine extracts from 6-, 12-, and 24-h-treated animals (Fig. 5A), there was no distinct staining in uterine sections from 6-h samples (not shown). Uterine cross sections from mice that had been treated for 12 h with estradiol exhibited nuclear staining in a portion of luminal epithelium (LE) cells (Fig. 6A, LE, see *arrow*), as well as in some stromal (Str) cells. This staining was not observed in serial sections stained with secondary antibody only (Fig. 6B), nor in specimens from mice treated for 12 h with ICI and estradiol together (Fig. 6C). Samples from 24-h estradiol treatment showed some faint epithelial staining as well as some positive Str cells (not shown).

DISCUSSION

Previous studies of the biological and biochemical responses of the uterus to acute E have indicated their biphasic nature (1, 2). Our study was designed to mimic the biological environment of the uterus subsequent to the preovulatory E surge and to determine whether the genomic response to acute estradiol would reflect the biphasic pattern. In general, we observed that the genomic response did mirror the physiological response, as unique clusters of genes characteristic of early or late responses were apparent (Fig. 1). Analysis of the genomic response from intervening time points illustrated that genes do indeed fall predominantly within the early or late clusters, rather than revealing intermediate clusters (Fig. 3). The relative lack of responses seen in αERKO samples indicates the dependence of most responses on ERα, whereas a response in the βERKO that is comparable to that of the WT illustrates a minimal role for ERβ. Similar observations regarding the relative roles of the ER isoforms in kidney and uterine tissues have been reported in microarray analysis employing chronic E treatment models (13, 14). One aspect of acute E dosing that our model has not yet addressed is the infiltration of the uterine tissue by immune cells, which will result in genomic changes in the total tissue RNA

Table 3. Fold Change Based on Microarray Data

Hours after E	0.5	2	6	12	24
Category/gene name					
Known estrogen regulated genes					
c-Fos	2.07	3.77			
Lactoferrin					4.56
SOX4		0.47			0.51
Cyr 61		4.35	2.15		
IGF signaling					
IGF-I			4.3	3.2	2.2
IGFBP3			0.35	0.25	0.28
IGFBP5					2
RAMP 3		5.56	10	5	2.7
Cell cycle					
p21	1.8	2.8	2.4	2.9	
Cyclin G				2.3	
MAD2		4.3	2.7		1.97
Stratifin					2.2
G1 to S phase transition 1				2.5	
cdc2					1.73
Chromatin					
H2A histone fmz			2.9	3.16	2.08
H1 histone fm2			0.55		
HDAC5			0.44	0.55	
Apoptosis					
BAD				2.7	2.03
IκBα	1.8				
AKT-1		1.95	2.1	2	
Wnt signaling					
Axin2 (Wnt signaling inhibitor)		1.7			
Expressed sequence AW227548 (fz-1)		0.5			
Casein kinase 1, α1		2.03			
ras Homolog gene family, member U (Wnt-1 responsive)		1.8			
Redox					
Thioredoxin 2		1.3	2.11	2.16	1.7
Thioredoxin reductase		1.3			2.15
Thioredoxin-interacting protein		0.4	0.34		0.33
Keratinization					
Small proline-rich protein 1A (cornifin)					3.6
Small proline-rich protein 2A (cornifin)				2.2	5.5
Stratifin					2.2
Transglutaminase 2			2.6	2.4	2
Keratin complex 1, acidic, gene 13					1.77
Keratin complex 1, acidic, gene 19					2.68
Keratin complex 2, basic, gene 6a					2.25
Keratoepithelin			0.37	0.25	0.22

samples that represent recruitment of new cell types rather than changes in transcription.

Previously Identified Estrogen Targets Validate Array Analysis

Predictably, the microarray data set included several uterine genes previously characterized as E responsive (see Table 3). The transcription factor c-*Fos*, which is known to be rapidly induced by estradiol (15), was induced as early as 30 min after estradiol treatment. *Lactotransferrin*, which is secreted by the epithelial cells into the lumen, is known to be robustly induced by estradiol (16), and was present in the late gene cluster. It was induced beginning 24 h after es-

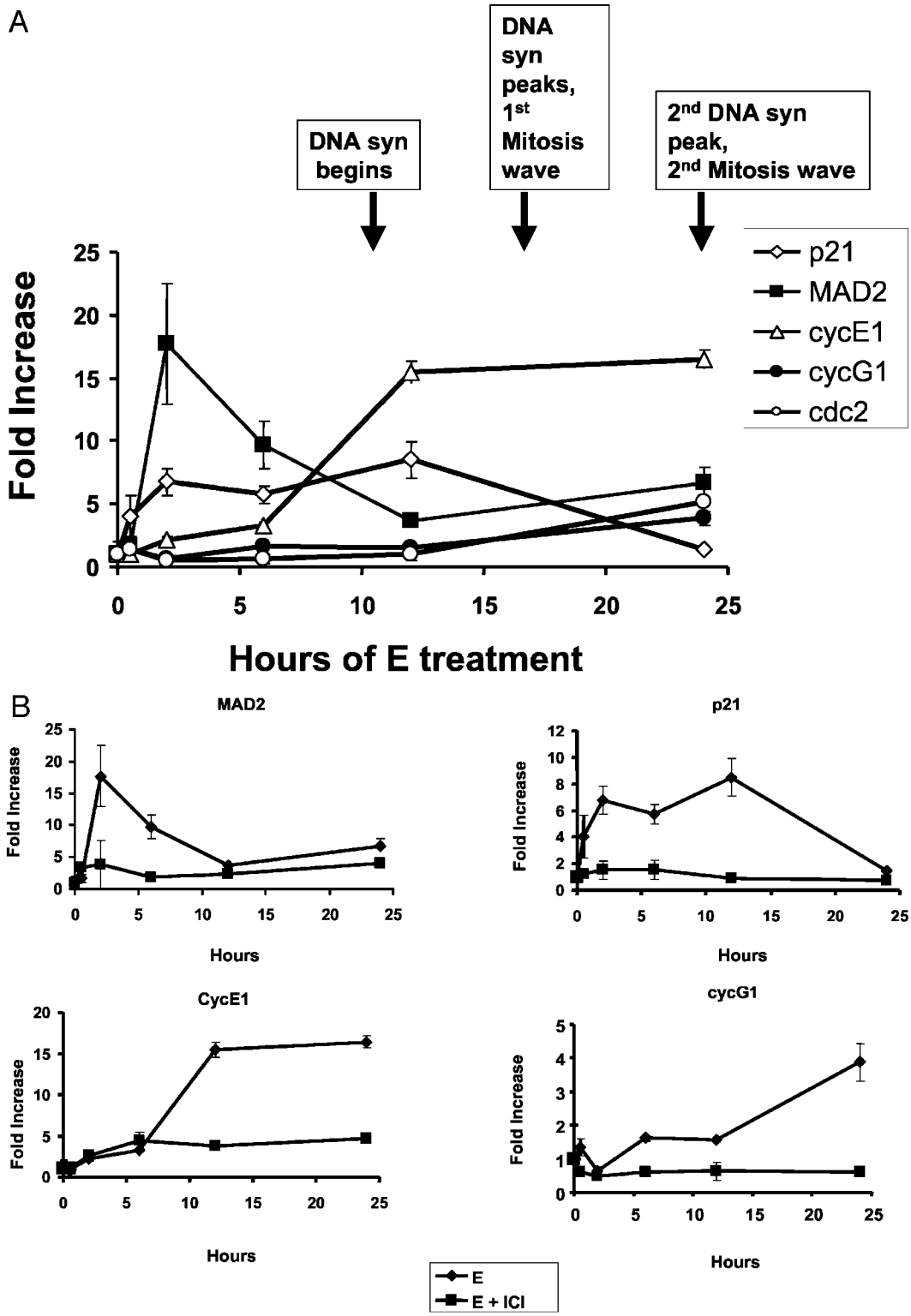

Fig. 4. Reverse Transcription and Real-Time PCR Analysis Verifies Regulation of Cell Cycle Modulators

Uterine RNA samples were prepared from ovx WT mice that were treated with estradiol or ICI and estradiol and collected at the same time points used for microarray analysis. cDNA was synthesized and used in a real-time PCR assay as described in *Materials and Methods*. Results were normalized to the *PL-7* transcript and expressed relative to the vehicle control, which was assigned the value 1.0. Each data point is the average ± SD of values obtained using three independent RNA samples for estradiol treated or two independent samples for ICI-treated samples and each sample was analyzed in triplicate. A, Time course of regulation of cell cycle modulators. *Arrows* indicate timing of biological events. B, Regulation and ICI inhibition of *MAD2, p21, cyclin E1, and cyclin G1*.

Table 4. Fold Change Measured by RT-Real-Time PCR

Hours after E	0.5	2	6	12	24
AKT 1	1.1	3.1	2.8	2.7	2.1
Cyclin D1	1.0	1.2	1.2	1.6	1.0
Histone H1 fm2	0.9	0.3	0.3	0.2	0.5
IκBα	2.6	2.4	2.4	1.7	1.6
RAMP3	2.1	31	45	27	10

RAMP3, Receptor (calcitonin) activity modifying protein 3.

tradiol injection. The transcription regulator SRY box-containing gene 4 (*SOX4*) has also previously been shown to be repressed in the mouse uterus after E treatment (17). Cysteine-rich protein 61 (*Cyr61*), an IGF binding protein (IGFBP)-like protein that has been reported to be E regulated and may play a role in cancer proliferation and progression (18–20), was also increased by estradiol in our uterine samples. Several components of the IGF signaling pathway were also regulated by estradiol. *IGF-1* and *IGFBP5* were both up-regulated, and *IGFBP3* was repressed by estradiol treatment (Table 3). The E regulation of these components in the mouse uterus has been previously reported (21–23). The recognition of these previously characterized E targets in our microarray data set serves as an indicator of the validity of our analysis method. Of these genes, only Cyr61 and IGFBP5 were induced in the αERKO uterus (Table 5), indicating that most of these genes are regulated by a conventional ERα-mediated pathway. It is especially interesting that, whereas IGFBP5 retained E responsiveness in the αERKO microarray analysis, it was not detected as regulated in the βERKO microarray analysis. Future studies to verify this observation might indicate whether IGFBP5 requires ERβ for regulation, or whether its expression is mediated by another mechanism. Similarly, SOX4, which is repressed by E at both 2 and 24 h in the WT samples, was repressed at 2 but not at 24 h in the βERKO. Future verification of this observation might indicate whether ERβ plays a role in maintenance of repression of this gene as well. Other genes known to be E regulated such as *progesterone receptor* and *creatine kinase B* were not represented on this chip [see http://dir.niehs.nih.gov/microarray/chips.htm for a complete list of genes on National Institute of Environmental Health Sciences (NIEHS) Mouse Chip version 1.0].

Novel Estrogen Targets and Pathways Identified by Microarray Analysis

Analysis of the many gene changes observed in this study indicated several functional categories that were regulated by E (Table 3). Additionally, because samples from various times after estradiol treatment were included, we were able to evaluate and compare the time course of potentially regulated genes in these pathways. For example several of the E-regulated genes were involved in chromatin structure or modification. *Histone H2A* mRNA expression increased 6 h following estradiol treatment, whereas *histone H1 family member 2* and *histone deacetylase 5* (*HDAC5*) were repressed. HDAC5 is generally associated with transcriptional repression (24, 25), and its suppression by estradiol treatment might alleviate its repressive activity, allowing transcription to proceed. Thus it is interesting that *HDAC5* transcription is down-regulated at 6 and 12 h (Table 3), as uterine RNA transcription in general is increasing (Table 1). Although proliferating tissue may in general require increased quantities of histones as the cell number increases, it is interesting that *histone H1 family member 2* levels are repressed (microarray data, Table 3; verified by RT-PCR, Table 4). Further verification and investigation of this observation might reveal an important function of chromatin in regulation of the biological response of the uterus to estradiol.

Components of the thioredoxin system, which regulate activities of enzymes and transcription factors by controlling their reduction state (26), were altered by estradiol (Table 3). *Thioredoxin*, and *thioredoxin reductase* were both up-regulated beginning 2 h after estradiol treatment, whereas *thioredoxin-interacting protein* was rapidly repressed.

Several genes involved in Wnt signaling were also E regulated. *Axin 2*, an inhibitor of β-catenin (27, 28), and thus of Wnt signaling, is induced 2 h following estradiol treatment. *Fz1*, a Wnt receptor that is activated by Wnt3a, 3 and 1 (29), is repressed at the same time point, suggesting suppression of Wnt signaling in the early phase of E response. *Casein kinase 1, α1*, which stabilizes β-catenin, (30–32) is also induced after 2 h of E treatment, as is the *ras homolog* gene family, member U (33), which is reported to be a Wnt responsive gene. The Wnt signaling pathway directs neonatal patterning of the uterus, and Wnts are expressed in the adult mouse uterus (34). Further investigation of Wnt signaling components that were identified as E regulated in this study has uncovered possible roles in uterine physiological response.

A number of genes associated with keratinization or cornification were also E regulated. *Small proline-rich protein 1A* and *small proline-rich protein 2A* (*cornifin* or *SPRR 1A* and *2A*) are both induced, *2A* beginning after 12 h, and *1A* beginning 24 h after estradiol treatment. Both of these molecules are cross-linked to keratin by *transglutaminase* (35, 36), which is induced by E beginning at the 6-h time point. *Stratifin*, which is expressed in keratinizing epithelia (37) and is also involved in G2/M control (38), is induced at 24 h. *Keratoepithelin*, also called TGFβ induced (68 kDa), is expressed in corneal epithelial cells (39), binds collagen I, II, and IV and is repressed by E beginning at 6 h. Several keratin complex molecules are induced by 24 h of E treatment as well. The keratinization of the vagina and cervix in response to E has been well studied (40), and the induction of these genes may reflect the inclusion of some cervical tissue in the uterine samples. It is interesting that keratoepithelin is

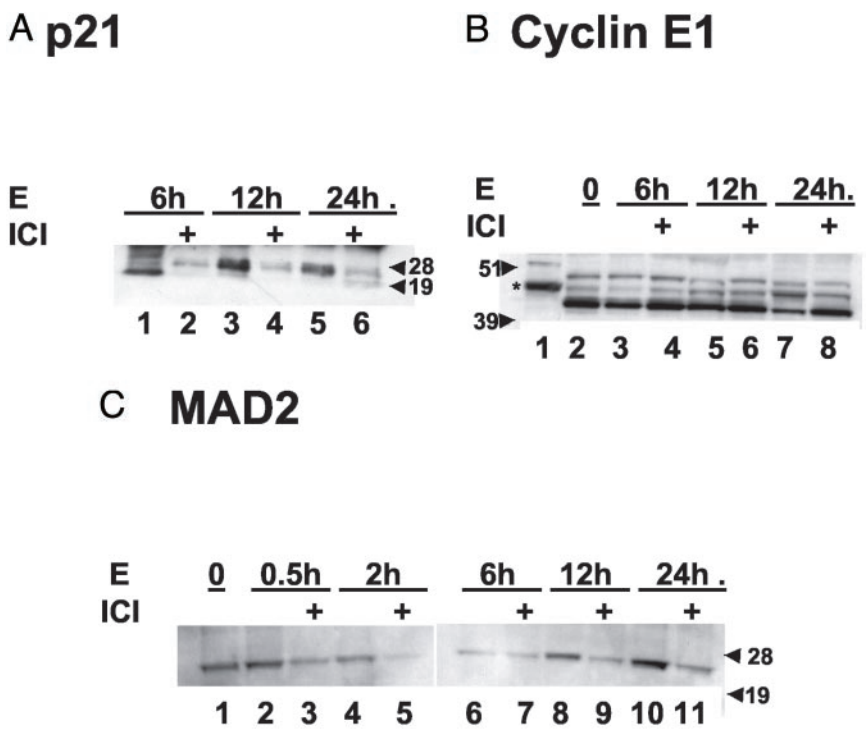

Fig. 5. Western Blot Shows Estrogen Regulation of Cell Cycle Proteins in Uterine Tissue

A, Fifty micrograms of total uterine protein were separated on a 10% NuPAGE gel. Transferred proteins were detected with an anti-p21 antibody. Samples were from mice treated with estradiol for 6 h (lanes 1 and 2), 12 h (lanes 3 and 4), or 24 h (lanes 5 and 6). Lanes 2, 4, and 6 were samples from mice also treated with the antiestrogen ICI. The size of protein standards (SeeBlue Plus2, Invitrogen), in kilodaltons, is indicated. Each lane is a pooled sample prepared from four to six mice. B, Fifty micrograms of total uterine protein were separated on a 10% NuPAGE gel. Transferred proteins were detected with an anticyclin E1 antibody. Lane 1 contains a control extract from human A431 cells treated with EGF, indicating the migration of human cyclin E1 (*). Samples were obtained from mice treated with vehicle (lane 2) or with estradiol for 6 h (lanes 3 and 4), 12 h (lanes 5 and 6) or 24 h (lanes 7 and 8). Lanes 4, 6, and 8 were samples from mice also treated with ICI. The sizes of protein standards in kilodaltons is indicated. Each lane is a pooled sample prepared from two mice. C, Fifty micrograms of total uterine protein were separated on a 12% NuPAGE gel. Transferred proteins were detected with an anti-MAD2 antibody. Samples were obtained from mice treated with vehicle (lane 1) or with estradiol for 0.5 h (lanes 2 and 3), 2 h (lanes 4 and 5), 6 h (lanes 6 and 7), 12 h (lanes 8 and 9), or 24 h (lanes 10 and 11). Lanes 3, 5, 7, 9, and 11 were samples obtained from mice also treated with ICI. The sizes of protein standards is indicated in kilodaltons. Each lane is a pooled sample prepared from four to six mice.

actually repressed, suggesting a role other than keratinization.

Apoptosis associated components were also E regulated. Bcl-associated death promoter (*BAD*), which stimulates apoptosis (41), was induced beginning 12 h after E treatment. Thymoma viral proto-oncogene 1, also called *AKT1*, a cell survival factor (42), showed increased RNA levels on the microarray (Table 3) that was verified by RT-PCR (Table 4), before the increase in *BAD*. The activity of the AKT 1 protein has been previously shown to be regulated by E (43); however, this analysis is the first to indicate that the transcription of *AKT1* is E regulated as well. *NF-κB* plays a critical role in inhibiting apoptosis (44). Interestingly, *IκBα* RNA was rapidly induced, and was only detected in the 30 min samples by microarray (Table 3), but remains elevated through 6 h and then declines according to RT-PCR analysis (Table 4). Estrogen withdrawal induces apoptosis in the uterus (45, 46), possibly to allow embryo invasion. The relative regulation of apoptosis genes in our study suggests E might coordinate the timing of apoptosis in the uterus. Future studies will indicate the significance of this finding to uterine physiology.

Receptor (calcitonin) activity modifying protein 3 (*RAMP3*), a protein that is involved in transport of calcitonin like receptors to the plasma membrane, and in modification of receptors to determine their ligand specificity (47, 48), was robustly and rapidly induced (Table 3), and this induction was verified by RT-PCR (Table 4). This protein has not been previously reported to be E regulated, and its induction suggests a possible role in calcitonin-like ligand signaling in preparation of the uterus for pregnancy, and warrants further investigation.

Estrogen Regulates Cell Cycle Modulators: Potential Role in Synchronous S Phase Progression

For the purposes of this initial report, we have further characterized the genomic response of several genes

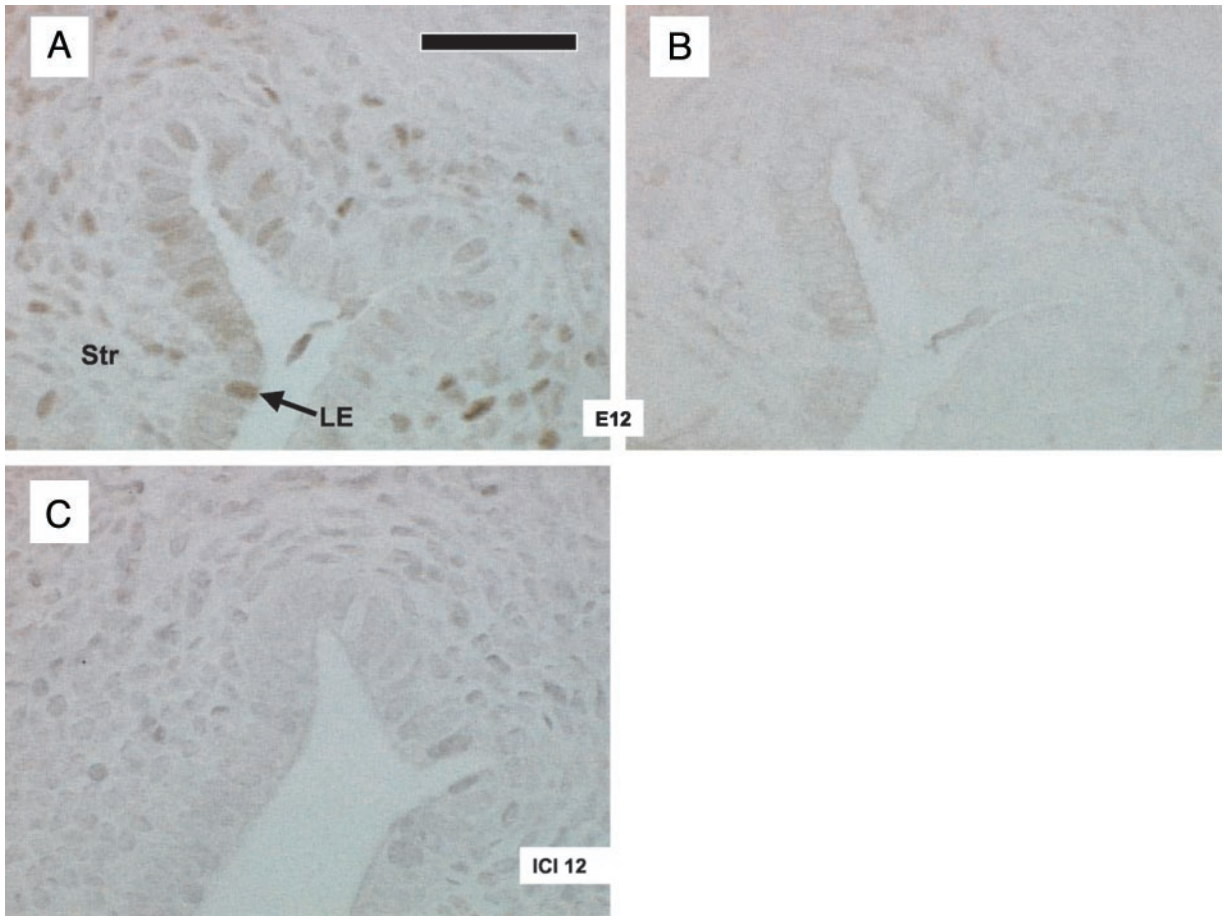

Fig. 6. p21 Protein Is Detected in Nuclei 12 h after Estradiol Treatment

p21 protein was detected in uterine samples from E-treated mice by immunohistochemistry. A and B, Serial sections from 12-h-estradiol-treated mice. C, From a mouse treated with ICI and estradiol for 12 h. A and C, Incubated with anti-p21 (1:10). B, Incubated with secondary antibody only. Each panel is representative of three to four individual samples. The *black bar* in panel A represents 40 μM. The LE and Str cells are labeled in panel A. The *arrow* shows a cell with positive nuclear staining.

Table 5. Fold Changes in Known Estrogen Targets in WT, αERKO, and βERKO Based on Microarray Data

	WT	αERKO	βERKO
c-fos (2 h)	3.8		3.5
Cyr 61 (2 h)	4.4	2.1	3.9
Lactoferrin (24 h)	4.6		2.7
SOX 4 (2 h)	0.47		0.46
(24 h)	0.51		
IGF-I (24 h)	2.2		2.2
IGFBP3 (24 h)	0.28		0.44
IGFBP5 (24 h)	2	1.7	

involved in cell cycle progression after acute E treatment. Regulation of these genes in this uterine model is not surprising, considering the coordinated increased uterine DNA synthesis and mitosis reported to begin 12–24 h following E treatment of ovx mice, indicative of synchronized entry into S phase (5). Thus, uterine epithelial cells must not only proliferate, but must do so at the proper time as the estrous cycle progresses, in preparation for implantation of embryos. Synchronous/coordinated regulation of the components modulating entry into S phase is one mechanism by which the acute exposure to the hormone estradiol might orchestrate this event. Estrogen regulation of some cell cycle modulators in the uterus has been previously reported. For example, E treatment induces nuclear relocalization of cyclin D1 protein and increase in expression of cyclins A and E proteins in the uterine epithelium (49). p21 protein expression has been shown to increase in the uterine LE 1–2 d after E treatment (50). It is especially interesting that p21, which inhibits progression into S phase, is maximally induced at both the RNA and protein levels (Figs. 4 and 5) and is localized to the nucleus 12 h following estradiol treatment (Fig. 6), just before the peak of entry into S phase, suggesting that the increased *p21* may prevent S phase progression of the epithelial cells until the proper time, allowing coordinated proliferation of the epithelial cells. Thus, the properly timed increase in *p21* may act as a gate, coordinating appropriate S phase progression.

Although *p21*-deficient mice exhibit normal fertility (51), other cdk inhibitors may compensate for the lack of *p21*. For example, the cdk inhibitor *p27*, which is not included on the microarray chip used for this study, is expressed in the uterus but is decreased after E treatment (49). Additionally, *p27*-deficient female mice are infertile due to both ovarian and uterine deficiencies (52), suggesting an essential role in the uterus. *p21* and *p18* (ink 4 family) were the only cdk inhibitors included on the microarray chip used in this study, and *p18* was not differentially expressed. Although *p18* is known to be important in male fertility, *p18*-deficient female mice are fertile (53). The uterine response of cdk-deficient mice (*p21, p18, p27*) to acute E dosing in terms of a properly timed coordinated increase in DNA synthesis has not yet been studied.

The moderate increase in *MAD2* transcript at 24 h (Fig. 4) and protein at 12–24 h (Fig. 5) as the epithelial cells prepare for mitosis at 16–24 h is consistent with the role of MAD2 in mitotic spindle assembly at the G2/M checkpoint (10). However, the almost 20-fold increase in *MAD2* transcript at 2 h as well as the presence of MAD2 protein in the vehicle and 30-min samples, when the cells are mitotically quiescent, is puzzling. Perhaps the early increase in MAD2 acts to delay progression past the G2/M checkpoint until all the molecules necessary for synchronous S phase entry have accumulated. Alternatively, the expression of MAD2 in nonmitotic cells might indicate a novel function for this protein.

Other Uterine Genomic Profiles

The model we applied in this study attempts to mimic the events just subsequent to the preovulatory estradiol surge, addressing a normal biological process. Several other studies of rodent uterine genomic response to E have been published; however, the study designs and biological issues addressed differed from ours. Naciff *et al.* (54) treated rat embryos with 17α-ethinyl estradiol or xenoestrogens on gestational d 11–20 and examined the genomic response in the developing reproductive tract as a model of embryonic exposure to estrogenic compounds. In another study, RNA was prepared from rat uterine RNA after 48 d of chronic treatment with estradiol and compared with vehicle-treated samples to identify E-regulated genes (23). In a third study, ovx rats or mice were treated with vehicle or E for 6 wk and uteri and kidneys collected for analysis to address the effect of chronic E treatment on gene expression (14). These three studies have in common a chronic exposure to E, unlike our study, which addresses a normal biological situation of events just subsequent to the preovulatory estradiol surge. In contrast, Reese *et al.* (55) attempted to address the biological situation that occurs at the time of implantation in the mouse uterus. As part of their analysis, a delayed implantation model was used whereby the ovaries were removed and replaced with progesterone to delay embryo implantation until estradiol replacement was given. Microarray analysis using these samples identified uterine genes induced 12 h following estradiol administration. Several genes they reported have been previously identified as E-regulated uterine genes or were also seen in our analysis, including *lactoferrin, MAD2, small proline rich protein 2A, cyclin E2, keratin complex 1, Histone H2A.1, and Cyr61.*

The advent and application here of microarray technology using a study design that mimics the physiological response of the reproductive tract to acute E has illustrated that the genomic response reflects the biphasic biological events. Additionally, application of this approach to transgenic α- and βERKO models indicated the genomic responses primarily require ERα. Finally, examination of the identities of other regulated gene families has suggested many new avenues of study that will enhance our understanding of the spectrum of mechanisms that influence the biological response of the uterus to acute E.

MATERIALS AND METHODS

Animals and Treatments

All animals were handled according to National Institutes of Health guidelines and in compliance with an NIEHS-approved animal protocol. Ovx C57 Bl/6 mice were purchased from Charles River (Raleigh, NC). In addition, αERKO or βERKO or WT littermates were obtained from Taconic Farms (Germantown, NY), and were ovx and housed for at least 10 d before studies to allow endogenous ovarian steroids to decrease. Groups of animals were treated with sesame oil vehicle (Sigma, St. Louis, MO), or with 1 μg estradiol (Steraloids, Newport, RI) either dissolved in 100 μl sesame oil and injected sc (6-, 12-, and 24-h groups) or 100 μl normal saline and injected ip (30-min and 2-h groups). Some animals were treated with 45 μg ICI (kindly provided by Zeneca Pharmaceuticals, Cheshire, UK) (dissolved in 50 μl dimethylsulfoxide injected ip) 30 min before estradiol injection. Animals were killed at the indicated times using CO_2 and the uterus was collected and weighed. In some cases, a portion of the uterus was fixed in 10% formalin (Fisher Scientific, Suwannee, GA), whereas the remainder was snap frozen in liquid nitrogen for later RNA or protein isolation.

Microarray Analysis

Frozen uterine tissue was pooled (at least five uteri per group), pulverized, then homogenized in Trizol (Invitrogen, Carlsbad, CA) and RNA was prepared according to the manufacturer's protocol. Isolated RNA was then further purified using the QIAGEN (Valencia, CA) Rneasy midi (100–500 mg RNA) or mini prep kit ($<$100 mg RNA) clean-up protocol.

Hybridizations and Data Analyses

A cDNA Mouse Chip (NIEHS Mouse Chip version 1.0), developed in-house at NIEHS, was used for gene expression profiling experiments. A complete listing of the genes on this chip is available at the following web site: http://dir.niehs.nih.gov/microarray/chips.htm. cDNA microarray chips were prepared according to DeRisi *et al*. (56). The spotted cDNAs were derived from a collection of sequence verified IMAGE

clones that covered the 5′ end of the gene and ranged in size from 500-2000 bp (Incyte Genomics, Palo Alto, CA). M13 primers were used to amplify insert cDNAs from purified plasmid DNA in a 100-μl PCR mixture. A sample of the PCR products (10 μl) was separated on 2% agarose gels to ensure quality of the amplifications. The remaining PCR products were purified by ethanol precipitation, resuspended in ArrayIt Spotting Solution Plus buffer (Telechem, San Jose, CA) and spotted onto poly-L-lysine coated glass slides using a modified, robotic DNA arrayer (Beecher Instruments, Bethesda, MD). Each total RNA sample (10 μg) was labeled with Cyanine (Cy) 3- or Cy5-conjugated deoxyuridine triphosphate (Amersham, Piscataway, NJ) by a reverse transcription reaction using the reverse transcriptase, SuperScript (Invitrogen, Carlsbad, CA), and oligo-deoxythymidine primers (Amersham). The fluorescently labeled cDNAs were mixed and hybridized simultaneously to the cDNA microarray chip. Each RNA pair was hybridized to at least four arrays, employing a fluor reversal accomplished by labeling the control sample with Cy3 in two hybridizations and with Cy5 in the other two hybridizations. The cDNA chips were scanned with either an Axon Scanner (Axon Instruments, Foster City, CA) or an Agilent Scanner (Agilent Technologies, Wilmington, DE) using independent laser excitation of the two fluors at 532- and 635-nm wavelengths for the Cy3 and Cy5 labels, respectively.

The raw pixel intensity images were analyzed using the ArraySuite version 2.0 extensions of the IPLab image processing software package (Scanalytics, Fairfax, VA). This program uses methods that were developed and previously described by Chen *et al.* (57) to locate targets on the array, measure local background for each target and subtract it from the target intensity value, and to identify differentially expressed genes using a probability-based method. The data were filtered to provide a cut off at the intensity level just above the buffer blank measurement values to remove from further analyses those genes having one or more intensity values in the background range. After pixel intensity, determination and background subtraction, the ratio of the intensity of the treated cells to the intensity of the control was calculated using Chen's method (57). Genes having normalized ratio intensity values outside of a 99% confidence interval were considered significantly differentially expressed. The lists of differentially expressed genes at the 99% confidence levels were created and deposited into the NIEHS Microarray Project System database (58). Any of these genes that indicated fluor bias or high variation were not considered for further analysis, and genes that were represented in 75% of the hybridization replicates were compiled for clustering. Clustering was conducted using the algorithm provided by Eisen (59).

The entire data are available at the web site http://dir.niehs.nih.gov/microarray/hewitt/.

Verification of Microarray Results by Real-Time RT-PCR

Ovx WT mice were treated as described for the microarray analysis, and RNA was prepared from mice treated with vehicle (20 mice) or 1 μg estradiol with (four mice per group) or without (six mice per group) pretreatment for 30 min with 45 μg of ICI and then collected 30 min, 2 h, 6 h, 12 h, or 24 after estradiol treatment. Uteri were frozen in liquid nitrogen, two uteri were pooled and pulverized, and RNA was prepared using Trizol reagent according to the manufacturer's protocol.

Reverse Transcription

To remove genomic DNA, RNA samples were incubated with 1 U of deoxyribonuclease I (DNaseI) (Invitrogen Corp.) per microgram of RNA for 15 min at room temperature. DNaseI was then inactivated by addition of 2.5 mM EDTA (pH 8.0) and heating at 65 C for 10 min. Reverse transcription of RNA (2 μg) using Superscript II (400 U) was carried out according to the manufacturer's instructions using oligo-deoxythymidine primers (Invitrogen Corp.). The resulting cDNA was treated with 4 U ribonuclease H (Invitrogen Corp.) for 20 min at 37 C to remove RNA:DNA hybrids. As a negative control, a sample containing RNA but no reverse transcriptase (minus RT) was also included. The resulting samples were diluted to 200 μl with DNase-free water. Ten microliters of this cDNA were used per well in 96-well plates for real-time PCR analysis.

Real-Time PCR Analysis

cDNA levels were detected using real-time PCR with the ABI PRISM 7700 Sequence Detection System (Applied Biosystems, Foster City, CA) and SYBR Green I dye. Primers were created using Applied Biosystems Primer Express Software version 2.0 (see supplemental Table 2). For cDNA amplification, 10 μl of cDNA was combined with 40 μl of a mixture containing SYBR Green PCR core reagents (Applied Biosystems, catalog no. 4304886) at the following concentrations: 1× PCR buffer, 4 mM $MgCl_2$, 50 nM each of deoxy (d) ATP, dCTP, dGTP, and deoxyuridine triphosphate, 0.5 U AmpErase uracil-N-glycosylase, 1.25 U AmpliTaq Gold DNA Polymerase, and 200 nM reverse and forward primers. Samples were analyzed in triplicate, and a minus RT sample was included with each plate to detect contamination by genomic DNA. Amplification was carried out as follows: 1) 50 C, 2 min (for uracil-N-glycosylase incubation); 2) 95 C, 10 min (denaturation); 3) 95 C, 15 sec, 60 C, 30 sec (denaturation/amplification). Dissociation curves were also created by adding the following steps to the end of the amplification reaction: 95 C, 15 sec (denaturation), 60 C, 20 sec, then gradually increasing to 95 C over 20 min finally holding at 95 C for 15 sec. Fold expression or repression was determined by quantitation of cDNA from target (E treated) samples relative to a calibrator sample (vehicle). For all samples, the gene for ribosomal protein 7 (rPL7) was used as the endogenous control for normalization of initial RNA levels. To determine this normalized value, $2^{-\Delta\Delta CT}$ values were compared between target and calibrator samples, where ΔCt = target gene (crossing threshold) Ct − rPL7 Ct, and $\Delta\Delta Ct = \Delta Ct_{control} - \Delta Ct_{treatment}$.

Western Blotting

Protein extracts were prepared by homogenization of a portion of the uterus, treated as described above, in homogenization buffer with added protease inhibitors and phosphatase inhibitors (Sigma) as in (60). Fifty micrograms of protein were loaded into each lane of NuPage (Invitrogen) 10% (p21 and cyclin E1) or 12% (MAD2) gels and proteins were separated and transferred to nitrocellulose membrane using the manufacturer's protocol and reagents. Membranes were stained with Ponceau S Solution (Sigma) to visualize equal protein loading and transfer (not shown). Mouse monoclonal antibodies against p21 were purchased from BD Pharminigen (San Diego, CA) and used at 1:500. Rabbit polyclonal antibody against MAD2 was generously provided by Dr. Salmon (University of North Carolina, Chapel Hill, NC) and used at 1:2500. Rabbit polyclonal antibody against cyclin E1 was purchased from Upstate Biotechnologies (Lake Placid, NY) and used at 2 μg/ml. Membranes were blocked with 5% milk in Tris-buffered saline (TBS)-Tween 20, then incubated with primary antibody diluted in 5% milk TBS-Tween, and finally in horseradish peroxidase (HRP)-conjugated secondary antibody [antirabbit HRP (Cell Signaling, Beverly, MA; 1:2000) , antimouse HRP (Amersham; 1:1000)], also diluted in 5% milk TBS-Tween. Bands were visualized with ECL reagent (Amersham) and Hyperfilm (Amersham).

Immunohistochemstry

Paraffin-embedded sections were deparaffinized in xylene, rehydrated in decreasing concentrations of ethanol, then processed in a decloaking chamber (Biocare Medical, Walnut Creek, CA) in Citrate buffer (Biocare) for 3 min. Endogenous peroxidase was blocked by incubation in 3% H_2O_2 for 10 min. p21 was detected using a mouse monoclonal antibody (sc 6246; Santa Cruz Biotechnology, Inc., Santa Cruz, CA) diluted 1:10 and Vector M.O.M. kit (Vector Laboratories, Burlingame, CA) and accompanying protocol with diethylaminobenzidine substrate.

Acknowledgments

We would like to thank Dr. Ted Salmon (University of North Carolina, Chapel Hill, NC) for providing the MAD2 antibody. We are grateful to James Clark, Page Myers, and Tracy Kingsley for the surgical procedures, and to Linwood Koonce and Vickie Walker for management of the ERKO colonies. We would also like to thank Drs. Edward Lobenhofer and Harriet Kinyamu for critically reading the study.

Received April 21, 2003. Accepted July 14, 2003.

Address all correspondence and requests for reprints to: Sylvia Curtis Hewitt, 111 Alexander Drive, MD E-01, Research Triangle Park, North Carolina 27709. E-mail: curtiss@niehs.nih.gov.

Current address for C.A.A.: Amgen Inc., Thousand Oaks, California 91320.

REFERENCES

1. Clark JH, Peck Jr EJ 1979 Female sex steroids. New York: Springer-Verlag
2. Katzenellenbogen BS, Bhakoo HS, Ferguson ER, Lan NC, Tatee T, Tsai TS, Katzenellenbogen JA 1979 Estrogen and antiestrogen action in reproductive tissues and tumors. Recent Prog Horm Res 35:259–300
3. Perez MC, Furth EE, Matzumura PD, Lyttle CR 1996 Role of eosinophils in uterine responses to estrogen. Biol Reprod 54:249–254
4. Griffith JS, Jensen SM, Lunceford JK, Kahn MW, Zheng Y, Falase EA, Lyttle CR, Teuscher C 1997 Evidence for the genetic control of estradiol-regulated responses. Implications for variation in normal and pathological hormone-dependent phenotypes. Am J Pathol 150: 2223–2230
5. Pollard JW, Pacey J, Cheng SV, Jordan EG 1987 Estrogens and cell death in murine uterine luminal epithelium. Cell Tissue Res 249:533–540
6. Couse JF, Korach KS 1999 Estrogen receptor null mice: what have we learned and where will they lead us? Endocr Rev 20:358–417
7. Sherr CJ 1994 G1 phase progression: cycling on cue. Cell 79:551–555
8. Horne MC, Goolsby GL, Donaldson KL, Tran D, Neubauer M, Wahl AF 1996 Cyclin G1 and cyclin G2 comprise a new family of cyclins with contrasting tissue-specific and cell cycle-regulated expression. J Biol Chem 271:6050–6061
9. Sherr CJ 1993 Mammalian G1 cyclins. Cell 73: 1059–1065
10. Shah JV, Cleveland DW 2000 Waiting for anaphase: Mad2 and the spindle assembly checkpoint. Cell 103: 997–1000
11. Hardwick KG 1998 The spindle checkpoint. Trends Genet 14:1–4
12. Yuen T, Wurmbach E, Pfeffer RL, Ebersole BJ, Sealfon SC 2002 Accuracy and calibration of commercial oligonucleotide and custom cDNA microarrays. Nucleic Acids Res 30:e48
13. Lindberg MK, Weihua Z, Andersson N, Moverare S, Gao H, Vidal O, Erlandsson M, Windahl S, Andersson G, Lubahn DB, Carlsten H, Dahlman-Wright K, Gustafsson JA, Ohlsson C 2002 Estrogen receptor specificity for the effects of estrogen in ovariectomized mice. J Endocrinol 174:167–178
14. Jelinsky SA, Harris HA, Brown EL, Flanagan K, Zhang X, Tunkey C, Lai K, Lane MV, Simcoe DK, Evans MJ 2003 Global transcription profiling of estrogen activity: estrogen receptor α regulates gene expression in the kidney. Endocrinology 144:701–710
15. Loose Mitchell DS, Chiappetta C, Stancel GM 1988 Estrogen regulation of c-fos messenger ribonucleic acid. Mol Endocrinol 2:946–951
16. Liu YH, Teng CT 1991 Characterization of estrogen-responsive mouse lactoferrin promoter. J Biol Chem 266: 21880–21885
17. Hunt SMN, Clarke CL 1999 Expression and hormonal regulation of the Sox4 gene in mouse female reproductive tissues. Biol Reprod 61:476–481
18. Rivera-Gonzalez R, Petersen DN, Tkalcevic G, Thompson DD, Brown TA 1998 Estrogen-induced genes in the uterus of ovariectomized rats and their regulation by droloxifene and tamoxifen. J Steroid Biochem Mol Biol 64:13–24
19. Sampath D, Winneker RC, Zhang ZM 2001 Cyr61, a member of the CCN family, is required for MCF-7 cell proliferation: regulation by 17β-estradiol and overexpression in human breast cancer. Endocrinology 142: 2540–2548
20. Xie D, Miller CW, O'Kelly J, Nakachi K, Sakashita A, Said JW, Gornbein J, Koeffler HP 2001 Breast cancer—Cyr61 is overexpressed, estrogen-inducible, and associated with more advanced disease. J Biol Chem 276: 14187–14194
21. Molnar P, Murphy LJ 1994 Effects of oestrogen on rat uterine expression of insulin-like growth factor-binding proteins. J Mol Endocrinol 13:59–67
22. Murphy LJ, Murphy LC, Friesen HG 1987 Estrogen induces insulin-like growth factor-I expression in the rat uterus. Mol Endocrinol 1:445–450
23. Andrade PM, Silva I, Borra RC, de Lima GR, Baracat EC 2002 Estrogen regulation of uterine genes *in vivo* detected by complementary DNA array. Horm Metab Res 34:238–244
24. Wade PA 2001 Transcriptional control at regulatory checkpoints by histone deacetylases: molecular connections between cancer and chromatin. Hum Mol Genet 10:693–698
25. Lemercier C, Verdel A, Galloo B, Curtet S, Brocard MP, Khochbin S 2000 mHDA1/HDAC5 histone deacetylase interacts with and represses MEF2A transcriptional activity. J Biol Chem 275:15594–15599
26. Nordberg J, Arner ES 2001 Reactive oxygen species, antioxidants, and the mammalian thioredoxin system. Free Radic Biol Med 31:1287–312
27. Lustig B, Jerchow B, Sachs M, Weiler S, Pietsch T, Karsten U, van de Wetering M, Clevers H, Schlag PM, Birchmeier W, Behrens J 2002 Negative feedback loop of Wnt signaling through upregulation of conductin/axin2 in colorectal and liver tumors. Mol Cell Biol 22:1184–1193
28. Leung JY, Kolligs FT, Wu R, Zhai Y, Kuick R, Hanash S, Cho KR, Fearon ER 2002 Activation of AXIN2 expression by β-catenin-T cell factor—a feedback repressor pathway regulating Wnt signaling. J Biol Chem 277: 21657–21665
29. Gazit A, Yaniv A, Bafico A, Pramila T, Igarashi M, Kitajewski J, Aaronson SA 1999 Human frizzled 1 interacts

with transforming Wnts to transduce a TCF dependent transcriptional response. Oncogene 18:5959–5966
30. McKay RM, Peters JM, Graff JM 2001 The casein kinase I family in Wnt signaling. Dev Biol 235:388–396
31. Peters JM, McKay RM, McKay JP, Graff JM 1999 Casein kinase I transduces Wnt signals. Nature 401:345–350
32. Sakanaka C, Sun TQ, Williams LT 2000 New steps in the Wnt/β-catenin signal transduction pathway. Recent Prog Horm Res 55:225–326
33. Tao W, Pennica D, Xu L, Kalejta RF, Levine AJ 2001 Wrch-1, a novel member of the Rho gene family that is regulated by Wnt-1. Genes Dev 15:1796–1807
34. Miller C, Pavlova A, Sassoon DA 1998 Differential expression patterns of Wnt genes in the murine female reproductive tract during development and the estrous cycle. Mech Dev 76:91–99
35. Marvin KW, George MD, Fujimoto W, Saunders NA, Bernacki SH, Jetten AM 1992 Cornifin, a cross-linked envelope precursor in keratinocytes that is down-regulated by retinoids. Proc Natl Acad Sci USA 89:11026–11030
36. Gibbs S, Fijneman R, Wiegant J, van Kessel AG, van De Putte P, Backendorf C 1993 Molecular characterization and evolution of the SPRR family of keratinocyte differentiation markers encoding small proline-rich proteins. Genomics 16:630–637
37. Leffers H, Madsen P, Rasmussen HH, Honore B, Andersen AH, Walbum E, Vandekerckhove J, Celis JE 1993 Molecular cloning and expression of the transformation sensitive epithelial marker stratifin. A member of a protein family that has been involved in the protein kinase C signalling pathway. J Mol Biol 231:982–998
38. Hermeking H, Lengauer C, Polyak K, He TC, Zhang L, Thiagalingam S, Kinzler KW, Vogelstein B 1997 14-3-3 Sigma is a p53-regulated inhibitor of G2/M progression. Mol Cell 1:3–11
39. Escribano J, Hernando N, Ghosh S, Crabb J, Coca-Prados M 1994 cDNA from human ocular ciliary epithelium homologous to β ig-h3 is preferentially expressed as an extracellular protein in the corneal epithelium. J Cell Physiol 160:511–521
40. Buchanan DL, Kurita T, Taylor JA, Lubahn DB, Cunha GR, Cooke PS 1998 Role of stromal and epithelial estrogen receptors in vaginal epithelial proliferation, stratification, and cornification. Endocrinology 139:4345–4352
41. Chao DT, Korsmeyer SJ 1998 BCL-2 family: regulators of cell death. Annu Rev Immunol 16:395–419
42. Datta SR, Brunet A, Greenberg ME 1999 Cellular survival: a play in three Akts. Genes Dev 13:2905–2927
43. Kelly MJ, Levin ER 2001 Rapid actions of plasma membrane estrogen receptors. Trends Endocrinol Metab 12: 152–156
44. Beg AA, Baltimore D 1996 An essential role for NF-κB in preventing TNF-α-induced cell death. Science 274: 782–784
45. Takagi-Morishita Y, Yamada N, Sugihara A, Iwasaki T, Tsujimura T, Terada N 2003 Mouse uterine epithelial apoptosis is associated with expression of mitochondrial voltage-dependent anion channels, release of cytochrome C from mitochondria, and the ratio of bax to bcl-2 or bcl-x. Biol Reprod 68:1178–1184
46. Monroe DG, Berger RR, Sanders MM 2002 Tissue-protective effects of estrogen involve regulation of caspase gene expression. Mol Endocrinol 16:1322–1331
47. Nikitenko LL, Brown NS, Smith DM, MacKenzie IZ, Bicknell R, Rees MC 2001 Differential and cell-specific expression of calcitonin receptor-like receptor and receptor activity modifying proteins in the human uterus. Mol Hum Reprod 7:655–664
48. McLatchie LM, Fraser NJ, Main MJ, Wise A, Brown J, Thompson N, Solari R, Lee MG, Foord SM 1998 RAMPs regulate the transport and ligand specificity of the calcitonin-receptor-like receptor. Nature 393:333–339
49. Tong W, Pollard JW 1999 Progesterone inhibits estrogen-induced cyclin D1 and cdk4 nuclear translocation, cyclin E- and cyclin A-cdk2 kinase activation, and cell proliferation in uterine epithelial cells in mice. Mol Cell Biol 19:2251–2264
50. Lai MD, Jiang MJ, Wing LY 2002 Estrogen stimulates expression of p21Waf1/Cip1 in mouse uterine luminal epithelium. Endocrine 17:233–239
51. Deng C, Zhang P, Harper JW, Elledge SJ, Leder P 1995 Mice lacking p21CIP1/WAF1 undergo normal development, but are defective in G1 checkpoint control. Cell 82:675–684
52. Fero ML, Rivkin M, Tasch M, Porter P, Carow CE, Firpo E, Polyak K, Tsai LH, Broudy V, Perlmutter RM, Kaushansky K, Roberts JM 1996 A syndrome of multiorgan hyperplasia with features of gigantism, tumorigenesis, and female sterility in p27(Kip1)-deficient mice. Cell 85: 733–744
53. Zindy F, den Besten W, Chen B, Rehg JE, Latres E, Barbacid M, Pollard JW, Sherr CJ, Cohen PE, Roussel MF 2001 Control of spermatogenesis in mice by the cyclin D-dependent kinase inhibitors p18(Ink4c) and p19(Ink4d). Mol Cell Biol 21:3244–3255
54. Naciff JM, Jump ML, Torontali SM, Carr GJ, Tiesman JP, Overmann GJ, Daston GP 2002 Gene expression profile induced by 17 α-ethynyl estradiol, bisphenol A, and genistein in the developing female reproductive system of the rat. Toxicol Sci 68:184–199
55. Reese J, Das SK, Paria BC, Lim H, Song H, Matsumoto H, Knudtson KL, DuBois RN, Dey SK 2001 Global gene expression analysis to identify molecular markers of uterine receptivity and embryo implantation. J Biol Chem 276:44137–44145
56. DeRisi J, Penland L, Brown PO, Bittner ML, Meltzer PS, Ray M, Chen Y, Su YA, Trent JM 1996 Use of a cDNA microarray to analyse gene expression patterns in human cancer. Nat Genet 14:457–460
57. Chen Y, Kamat V, Dougherty ER, Bittner ML, Meltzer PS, Trent JM 2002 Ratio statistics of gene expression levels and applications to microarray data analysis. Bioinformatics 18:1207–1215
58. Bushel PR, Hamadeh H, Bennett L, Sieber S, Martin K, Nuwaysir EF, Johnson K, Reynolds K, Paules RS, Afshari CA 2001 MAPS: a microarray project system for gene expression experiment information and data validation. Bioinformatics 17:564–565
59. Eisen MB, Spellman PT, Brown PO, Botstein D 1998 Cluster analysis and display of genome-wide expression patterns. Proc Natl Acad Sci USA 95:14863–14868
60. Hewitt SC, Goulding EH, Eddy EM, Korach KS 2002 Studies using the estrogen receptor α knockout uterus demonstrate that implantation but not decidualization-associated signaling is estrogen dependent. Biol Reprod 67:1268–1277